Remote Sensing of Environment 115 (2011) 2954–2964

Contents lists available at ScienceDirect

Remote Sensing of Environment

journal homepage: www.elsevier.com/locate/rse

Measuring effective leaf area index, foliage profile, and stand height in New England forest stands using a full-waveform ground-based lidar

Feng Zhao [a,*], Xiaoyuan Yang [a], Mitchell A. Schull [a], Miguel O. Román-Colón [a], Tian Yao [a], Zhuosen Wang [a], Qingling Zhang [a], David L.B. Jupp [b], Jenny L. Lovell [b], Darius S. Culvenor [c], Glenn J. Newnham [c], Andrew D. Richardson [d], Wenge Ni-Meister [e], Crystal L. Schaaf [a], Curtis E. Woodcock [a], Alan H. Strahler [a]

[a] Department of Geography and Environment, Boston University, Boston, MA 02215, USA
[b] CSIRO Marine and Atmospheric Resources, Canberra ACT 2601, Australia
[c] CSIRO Sustainable Ecosystems, Clayton South, Victoria 3169, Australia
[d] Department of Organismic and Evolutionary Biology, Harvard University, Cambridge, MA 02138, USA
[e] Department of Geography, Hunter College of CUNY, New York, NY 10021, USA

ARTICLE INFO

Article history:
Received 4 March 2009
Received in revised form 26 August 2010
Accepted 31 August 2010
Available online 29 April 2011

Keywords:
LAI
Lidar
Foliage profile
Height
Hemispherical photograph
LAI-2000
LVIS
New England

ABSTRACT

Effective leaf area index (LAI) retrievals from a scanning, ground-based, near-infrared (1064 nm) lidar that digitizes the full return waveform, the Echidna Validation Instrument (EVI), are in good agreement with those obtained from both hemispherical photography and the Li-Cor LAI-2000 Plant Canopy Analyzer. We conducted trials at 28 plots within six stands of hardwoods and conifers of varying height and stocking densities at Harvard Forest, Massachusetts, Bartlett Experimental Forest, New Hampshire, and Howland Experimental Forest, Maine, in July 2007. Effective LAI values retrieved by four methods, which ranged from 3.42 to 5.25 depending on the site and method, were not significantly different ($\beta < 0.1$ among four methods). The LAI values also matched published values well. Foliage profiles (leaf area with height) retrieved from the lidar scans, although not independently validated, were consistent with stand structure as observed and as measured by conventional methods. Canopy mean top height, as determined from the foliage profiles, deviated from mean RH100 values obtained from the Lidar Vegetation Imaging Sensor (LVIS) airborne large-footprint lidar system at 27 plots by −0.91 m with RMSE = 2.04 m, documenting the ability of the EVI to retrieve stand height. The Echidna Validation Instrument is the first realization of the Echidna® lidar concept, devised by Australia's Commonwealth Scientific and Industrial Research Organization (CSIRO), for measuring forest structure using full-waveform, ground-based, scanning lidar.

1. Introduction

Leaf area index (LAI), foliage profile (leaf area with height), and stand height are critical vegetation structural parameters for biogeoscience applications. This is especially true of leaf area index, which is used in carbon balance modeling and in the surface radiation balance modules of regional and global climate models (Hyde et al., 2006). In mapping the spatial variation in leaf area index as input to spatially distributed-parameter models, LAI is typically derived by regressions between ground-truth LAI and spectral or angular information from airborne or satellite imagery (Jensen et al., 2008; Breda, 2003; Myneni et al., 2002; Clark et al., 2008). As a result, the accuracy of LAI estimates over landscapes depends heavily on the accuracy of ground-based measurements of LAI.

The major methodologies for ground-based measurement of LAI generally fall into two groups: direct measures, including destructive sampling, litterfall collection, or point contact sampling; and indirect measures, including hemispherical photos and specially designed optical instruments such as the LAI-2000 Plant Canopy Analyzer (Li-Cor, Inc.), AccuPAR Light Interception Device (Decagon Devices, Inc.), or TRAC instrument (Tracing Radiation and Architecture of Canopies, 3rd Wave Engineering) (Jonckheere et al., 2004). While accurate LAI measurements can be made by direct methods for small-stature vegetation such as agricultural crops and plantations (Chen et al., 1997), LAI measurements of natural forest ecosystems often rely on indirect methods because direct measurement of forest LAI is costly and time-consuming (Weiss et al., 2004).

Indirect methods of LAI retrieval generally use optical methods that rely on identifying the gaps within the canopy through which the sky can be seen. They use gap probability to retrieve "effective LAI" with a model of negative exponential attenuation of the ray beam along a path through the canopy coupled with a model of leaf angle distribution calibrated by gap probability with zenith angle. Because

* Corresponding author. Tel.: +1 617 353 8031.
E-mail address: zhao26@bu.edu (F. Zhao).

0034-4257/$ – see front matter © 2011 Elsevier Inc. All rights reserved.
doi:10.1016/j.rse.2010.08.030

the ray beam can be intercepted by fine and coarse branches as well as leaves, the effective LAI includes branches and is sometimes referred to as a "plant area index". Clumping of foliage into leaf clusters (e.g., broadleaf clusters or conifer shoots) and the clumping of leaf clusters into tree crowns also influences the effective LAI (Chen & Black, 1992; Chen & Cihlar, 1995; Chen et al., 2006). Optical methods that measure the spatial distribution of gaps (e.g., TRAC) are sometimes used to retrieve a clumping index to correct the effective LAI for this effect.

This paper focuses on a ground-based, near-infrared, scanning lidar, the Echidna Validation Instrument, built by Australia's Commonwealth Scientific and Industrial Research Organization (CSIRO), that retrieves effective LAI, foliage profile, stand height, and other forest structural parameters from digitized, full-waveform, lidar returns (Jupp et al., 2009; Strahler et al., 2008). The EVI is the first realization of a concept for measuring forest structure using full-waveform, under-canopy, scanning lidar devised by Australia's Commonwealth Scientific and Industrial Research Organization (CSIRO). The concept is patented using the trademark Echidna in Australia, the United States, New Zealand, China, Japan and Hong Kong with patents in other countries pending.[1]

A number of previous studies have utilized lidar for retrieval of leaf area index. Most of these have utilized small-footprint (footprint <1 m) airborne lidar systems that return the distance to the first or first and last scattering events, and acquire counts of scattering events by height above the ground to determine the fraction of leaf area with depth (Magnussen & Boudewyn, 1998; Riaño et al., 2004; Parker et al., 2004; Morsdorf et al., 2006; Hilker et al., 2010). However, this approach is limited by the inability to differentiate canopy returns from ground returns. A strength of the airborne approach is its ability to cover and map large areas.

In contrast to first-return lidars, the ground-based lidar scanner we describe in this paper samples the scattering returned by the entire laser pulse as it passes through the canopy. By scanning, it also acquires observations over a wide range of zenith angles (±130°) and azimuth angles (0°–360°) at a fine angular resolution. Jupp et al. (2005, 2009) described the theory for the retrieval of LAI and foliage profile from Echidna lidar and demonstrated its application using data acquired by the EVI at the Bago-Maragle Forest, New South Wales, Australia, in a ponderosa pine plantation and a natural, but managed, stand of eucalypts. Strahler et al. (2008) further validated retrieval of EVI-derived forest structural parameters, such as mean stem diameter and stem count density (trees per hectare), with ground truth data collected at the same location.

While previous studies have demonstrated the ability of the EVI to measure the effective leaf area index of conifer and broadleaf forest stands, the consistency of these retrievals with those of alternative optical methods has not yet been assessed. The objective of this research is to examine that consistency by comparing LAI values retrieved by the EVI and those using hemispherical photography and the LAI-2000 Plant Canopy Analyzer for six stands representing a typical range of New England forests. We also retrieve the foliage profile and compare stand heights obtained from EVI data with data obtained by the Laser Vegetation Imaging Sensor (LVIS), a large-footprint airborne lidar research instrument operated by NASA Goddard Space Flight Center (Blair et al., 1999, 2006).

Comparison of LAI retrievals is limited by not having an accurate reference standard. That is, we do not present direct measurements of LAI that would, in principle, be more accurate than our optical retrievals. Without such "ground truth," our experimental design is to compare LAI retrievals from EVI with those of hemispherical photos and the LAI-2000 to see if they are statistically different. If not, we conclude that the EVI provides LAI retrievals comparable to those obtained by hemispherical photography and the LAI-2000.

[1] US patent No 7,187,452, Australian Patent No. 2002227768, New Zealand Patent 527547.

In this circumstance, the statistical significance lies in the power of the test to accept the null hypothesis, rather than in the probability that the null hypothesis may be rejected. The power with which we accept the null hypothesis depends on the sample size and the inherent variance in the measurements. Neither of these is easily controlled in our situation. The amount of field time and data acquisition is fixed by budgetary constraints, and the inherent variance is a function of the actual forest stands that are measured. However, the powers of the actual tests performed were largely sufficient to determine whether all methods achieved similar results.

1.1. Study area

Data from the EVI and ground measurements were acquired in July 2007 at three hardwood and three conifer stands of varying stocking densities at Harvard Forest, Massachusetts; Bartlett Experimental Forest, New Hampshire; and Howland Experimental Forest, Maine. A brief description of each forest site and its dominant species composition is given in Table 1. Within each site, our measurements were acquired within a 1 ha area of 100 by 100 m in which we laid out five plots of 20 m radius (25-m radius at the Harvard hardwood site) (Fig. 1a). In each plot, we located trees by distance and azimuth from the center point and measured and recorded their structural attributes (e.g., species, diameter at breast height, tree height, and crown form), acquired one or more EVI scans, and observed LAI with the LAI-2000 and with hemispherical photos (13 observations per plot) (Fig. 1b). At the Bartlett site and Howland site, some LAIs had been previously measured with LAI 2000 on the plots by our independent collaborators.

1.2. Echidna Validation Instrument

The EVI utilizes an infrared laser source (1064 nm) that emits a beam of 15 ns pulses at a frequency of 2 kHz that can generate a usable return from a distance of 100 meters or more in medium density forests. The instrument's optical system provides a beam diameter of 29 mm with a manually variable divergence of 2–15 mrad. By adjusting the beam divergence and the scanning rate, the entire field of view can be covered without gaps at varying angular resolutions. The laser pulse width is 14.9 ns (full-width-half-maximum, FWHM), which corresponds to about 2.4 m in range. The pulse power is sharply peaked to provide accurate range to hard targets.

The instrument scans the field of view using a rotating 45°-angled mirror that directs the beam in a vertical plane to cover zenith angles of ±130° while the instrument base rotates through 180° to provide full azimuthal coverage. The return sensor system records the full return waveform using a selectable sampling rate of up to 2 G samples per second. The maximum sampling rate corresponds to a resolution in range of about 7.5 cm, which is well within the FWHM of the pulse so that all return signals above the noise level are sensed. Encoding is linear, so that the sensor response can be calibrated in power units. More information on the EVI and its early trials can be found in Jupp et al. (2005).

Table 1
Site characteristics.

Site name	Species group	Leading dominants	Mean basal area, m^2/ha
Harvard hardwood	Hardwood	Red maple, red oak, birch	34.46
Harvard hemlock	Conifer	Hemlock, red maple	55.48
Bartlett B2	Hardwood	Red maple, beech, ash	44.96
Bartlett C2	Hardwood	Red maple, beech, birch	40.66
Howland main tower	Conifer	Red spruce, hemlock, white pine	55.36
Howland shelterwood	Conifer	Red spruce, hemlock	26.50

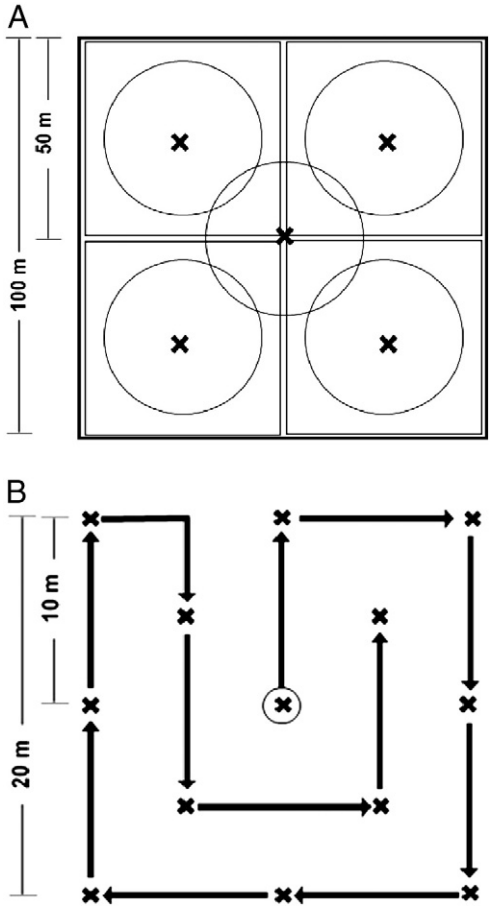

Fig. 1. Sample layout. (A) Sample layout for EVI scans. Five EVI scans were acquired at each site. (B) Sample layout for LAI-2000 observations and hemispherical photographs. At each scan point, 13 LAI-2000 and hemispherical photo measurements were acquired in the pattern shown with the scan point circled as the starting point. Arrows indicate the walking path for the instrument operator.

Because the Echidna lidar digitizes the intensity of the pulse reflected from targets along the entire transmission path, the data have three dimensions: zenith angle, azimuth angle, and range. However, there is considerable data redundancy, since all scans converge at the zenith. As a result, the data are averaged within equal-angle bins, leading to a *plate carreé* projection that we refer to as the Andrieu projection after its use by Andrieu et al. (1994).

1.3. Hemispherical photography

The hemispherical canopy photograph provides a commonly-used, indirect optical method to obtain leaf area index and canopy transmittance based on gap fractions derived from light attenuation within the canopy as measured by the contrast between sky and canopy elements (Hale & Edwards, 2002). In this study, a Nikon Coolpix 900 camera with a 180° fisheye lens pointed toward the zenith was used at a resolution of 1391×1405. All photographs were taken before sunrise or after sunset under clear sky conditions to ensure homogeneous, shadow-free illumination of the canopy and high contrast in the blue spectral region between the canopy and the sky. To properly sample the spatial variability over the site, 13 hemispherical photographs were taken at a spacing of 10 m at each plot following the sample design in Fig. 1. Exposures were not always optimal, due to operational problems, but nearly all frames were usable. All digital photographs were collected as highest-quality JPEG images and were analyzed using HemiView software (Dynamax, Inc., Houston, TX).

1.4. LAI-2000 instrument

The LAI-2000 Plant Canopy Analyzer (Li-Cor Inc., 1992) is a portable instrument that provides LAI estimates by measuring radiation received by a fish-eye optical sensor in five zenith angle ranges under a forest canopy and comparing them to reference measurements of skylight collected simultaneously or contemporaneously in a nearby open area. Radiation is filtered to remove wavelengths above 490 nm, i.e., retaining a blue band in which the sky is bright due to Rayleigh scattering and vegetation is dark due to chlorophyll absorption.

In this study, we operated the LAI-2000 in one-instrument mode, starting and ending with reference readings of unobstructed skylight that were linearly scaled with time to match under-canopy readings. Data acquired by our collaborators at Bartlett site and Howland tower site used two-instrument mode, in which a second instrument simultaneously recorded skylight continuously at a remote location. LAI-2000 observations in our study used the same observation plan as hemispherical canopy photographs (Fig. 1b), but measurements by our collaborators at Bartlett and Howland sites used a 100-m transect with data acquired at 10-m intervals.

2. Methodology

Most indirect measurements of LAI are inferred from measurement of radiation transmission through crowns, specifically gap fraction (Ross, 1981). The gap fraction represents the probability that a ray beam will have no contact with vegetation elements during the transmission process (Weiss et al., 2004). The theory for retrieving leaf area index from gap probability with height as determined by optical methods is well-established in the literature (Wilson, 1963; Miller, 1967). Assuming a random spatial distribution of leaves (spherical leaf angle distribution), an effective LAI that is not corrected for clumping or for the presence of branches can be calculated from the gap fraction by utilizing the exponential relationship between gap fraction and LAI. Thus, accurate gap fraction measurement is of particular importance for indirect retrieval of leaf area index.

2.1. Gap fraction

The essence of widely-used light extinction models are gap fractions as a function of zenith angle, which can be calculated as follows:

$$P(\theta) = \frac{P_s}{P_s + P_{ns}} \quad (1)$$

where θ is a zenith angle or a small range of zenith angles of all azimuths called a zenith ring; $P(\theta)$ is the gap fraction at θ; P_s is the fraction of sky at θ; and P_{ns} is the fraction of vegetation (leaf and branch) at θ. Unlike hemispherical photos and EVI data, which can be processed to provide gap fraction within a large number of zenith and azimuth angle ranges, the LAI-2000 calculates effective leaf area index based on the transmittance in five fixed-view-angle sectors.

2.2. Hemispherical photography

For processing of the hemispherical photos, the blue channel is generally chosen for maximum contrast between leaf and sky. The gap fraction is derived by thresholding a gray-level image to distinguish leaf from sky. Selection of the optimal brightness threshold therefore becomes one of the main problems in the literature of hemispherical photographs for determination of LAI (Jonckheere et al., 2005; Wagner,

2001). Although manual thresholding can produce a bias (Frazer et al., 2001), we used the analyst-determined thresholding method for its flexibility, given the wide range of exposure conditions and image qualities that were present in the data.

2.3. Apparent reflectance and gap probability from Echidna lidar returns

In processing EVI data, we transform the instrument's returned-power measurements to apparent reflectance (Jupp & Lovell, 2007; Jupp et al., 2009), described as the reflectance of a large diffuse target normal to the beam that would return the same power at range as the actual target.

$$\rho_{app}(r) = \frac{r^2 E(r) - e}{C(r)\ T_A^2\ E_0} = \rho_v\ P_{FC}(r) = -\rho_v\ \frac{dP_{gap}}{dr}(r) \tag{2}$$

where r is the range; $C(r)$ is the target optics calibration factor at range r; $E(r)$ is the measured power at range r; E_0 is the signal energy at source; T_A is the atmospheric transmission; e is the background signal power; ρ_v is the effective volume reflectance; $P_{FC}(r)$ is the probability of first contact at range r; and $P_{gap}(r)$ is the probability of gap between the source and a point at range r. We define a gap probability $P_{gap}(\theta, r)$ as

$$P_{gap}(\theta, r) = 1 - \frac{1}{\rho_a}\int \rho_{app} r' dr' \tag{3}$$

where ρ_a is the normal reflectance of a facet.

The P_{gap} in Eq. (3) at the farthest range is derived from the sum of the apparent reflectances at each range scaled by the normal reflectance of the leaf. This assumes that leaf reflectance and leaf angle distribution are isotropic. If they are not, apparent reflectances will be larger or smaller by a value related to the way in which the directional reflectance of the leaf interacts with the leaf angle distribution (i.e., a canopy "phase" effect, Jupp et al., 2009). To remove this effect, it is necessary to rescale the P_{gap} image so that $P_{gap} = 0$ for fully intercepted targets, $P_{gap} = 1$ for pure sky shots, and P_{gap} for partially intercepted shots is scaled between 0 and 1. Fig. 2a shows an image of P_{gap} at far range obtained by processing an EVI scan in this way.

In the leaf canopy, the model for the gap probability as a function of height in a given direction as measured by the zenith angle θ is:

$$P_{gap}(\theta) = e^{-\Omega(\theta)G(\theta)L/\cos(\theta)} \tag{4}$$

where L is the leaf area index; $G(\theta)$ is the fraction of the leaf area projected on a plane normal to the zenith angle θ (Ross G-function, Ross, 1981); and Ω is a clumping index determined by the spatial distribution of leaves. Here we assume the clumping index is isotropic, but some recent work has treated the clumping index as a function of zenith angle (Leblanc, 2002; Leblanc et al., 2005).

Thus, if the clumping index were known, the leaf area index L could be retrieved from the gap probability as:

$$L = \frac{-\log P_{gap}(\theta)\cos(\theta)}{\Omega G(\theta)}. \tag{5}$$

Since the clumping index is generally not known, most methods analyze the data as if $\Omega = 1$ and call the resulting estimate the effective LAI. This can be regarded as a value close to the average $L_{eff} = \overline{\Omega L}$. As noted earlier, effective LAI values retrieved by optical methods, including the Echidna lidar, will normally include the area of twigs and fine branches.

2.4. LAI and foliage profile retrievals with the Echidna Validation Instrument

Following Jupp et al. (2009), we used two methods to estimate effective LAI: single direction and multiple directions. Since the G-function can be considered as independent of leaf inclination at a

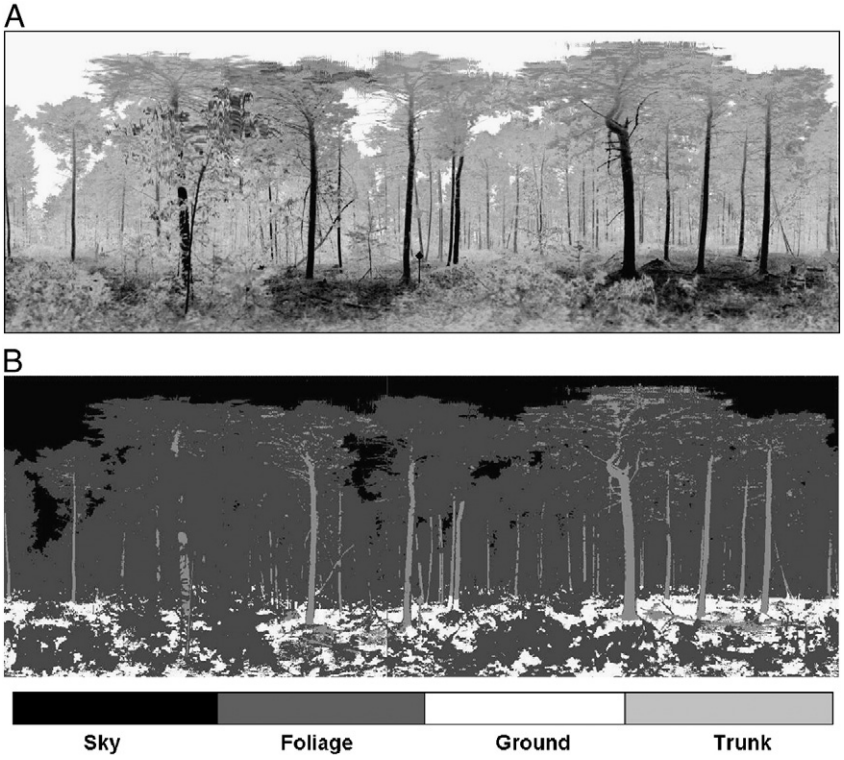

Fig. 2. (A) Gap probability at far range (60 m), shown in gray scale from 0 (black) to 1.0 (white). (B) Trunk and foliage separation. Black, sky; white, ground; light gray, trunk or branch; dark gray, leaves.

"hinge angle" of $\theta \approx \tan^{-1}(\pi/2) = 57.5°$ (Wilson, 1963), LAI can be approximated as:

$$L \approx -1.1 \log\left(P_{gap}(57.5°)\right). \quad (6)$$

This is referred to as the "hinge angle" method, and we apply it to EVI P_{gap} values for the zenith ring 55–60°.

Effective LAI can also be retrieved with a simple regression method (Jupp et al., 2009) from multiple view directions using the model:

$$L_h + L_v X(\theta) \approx -\log P_{gap}(\theta, H) \quad (7)$$

where H is the top height of the canopy; $X(\theta) = (2/\pi)\tan\theta$; $L = L_h + L_v$; and L_h and L_v are horizontal and vertical components of the LAI. L_h and L_v are then estimated by regression over zenith rings from 5 to 65°. The zenith ring 0–5° is omitted since the Echidna is typically positioned no closer than 2 m from the nearest large tree, thus causing the overhead ring to show a small bias toward lower P_{gap} values.

Secondly, to overcome the variation in the single-angle estimate of foliage profile, Jupp et al. (2009) suggested a solid-angle-weighted profile that reflects the unbiased average. The average normalized foliage profile $f(z)$ is defined as follows:

$$\frac{L(z)}{LAI} = \frac{\log P_{gap}(\theta, z)}{\log P_{gap}(\theta, H)}$$
$$f(z) = LAI \frac{\partial}{\partial z}\left(\frac{\log P_{gap}(\theta, z)}{\log P_{gap}(\theta, H)}\right). \quad (8)$$

In Eq. (8), the notation $\bar{\theta}$ indicates that the normalized data are averaged over a zenith ring (i.e., not a mean angle as the bar symbol might imply).

2.5. LAI retrieval using HemiView software

For retrieval of leaf area index from hemispherical photos, Poisson models in one form or another are typically used. The HemiView software uses an approach proposed by Campbell (1986). In this model, an extinction coefficient k is defined as:

$$k = \frac{\left(x^2 + \tan^2\theta\right)^{\frac{1}{2}}}{x + 1.774(x + 1.182)^{-0.733}}$$
$$LAI = \log\left(P_{gap}\right)/k \quad (9)$$

where θ is the zenith angle and x is the ellipsoidal leaf angle distribution parameter (ELADP). The software finds values of k and x that best fit the measured gap fraction values derived from the hemispherical photographs and then finds the (effective) LAI.

In this study, 13 images for each plot were processed using the HemiView software. It segments the sky hemisphere into zenithal rings and azimuthal sectors, and then removes any zenithal–azimuthal segments with null gaps or full gaps to allow azimuthal computation of LAI for each segment (Lang & Xiang's method, 1986). Thus, the average values from a single image are computed as

$$\overline{\mathrm{LAI}} = \frac{1}{n}\sum_1^n LAI_a \quad (10)$$

where LAI_a are sectorial values and n is the number of azimuthal sectors. The mean LAI can therefore better account for azimuthal heterogeneity in the canopy (Walter & Torquebiau, 2000), which also compensates for some effects of clumping.

2.6. LAI retrieval using the LAI-2000

By comparing radiation measurements under the canopy with unobstructed sky measurements, the LAI-2000 instrument determines canopy light interception in five zenith bands centered at angles of 7°, 23°, 38°, 53°, and 68°. LAI is then estimated by inversion of a Poisson model using Miller's formula as approximated by Welles and Norman (1991).

$$L = -2\sum_i \ln T_i \cos\theta_i W_i \quad (11)$$

where i = 1–5 zenith bands; T_i is the transmission in the ith band; and W_i are weighting factors. In addition, to avoid LAI underestimates due to scattering of blue light by leaves in outer rings, LAI is calculated from the slope and intercept of a plot of mean contact number against band center angle in radians (Lang, 1987). The LAI is then taken as twice the sum of the slope and intercept. In this study, the LAI is computed based on the Eq. (11). As noted earlier, this is effective LAI, which contains non-leaf area and includes the effects of clumping.

2.7. Trunk and foliage separation with Echidna lidar

Since nonphotosynthetic components of forest canopies, including branches and boles, also intercept varying amounts of light, they contribute to the LAI derived from the gap fraction method, leading to the overestimation of LAI. Thus, the amount of canopy shading from woody structures needs to be assessed to remove the contribution of this nonphotosynthetic component. Generally, an index termed the woody-to-total area ratio is used (Helena et al., 2005):

$$L = (1-\alpha)L_e \quad (12)$$

where α is the woody-to-total area ratio and L_e is the effective leaf area index. The woody-to-total area ratio can be obtained directly from destructive sampling; indirectly from allometric methods; by differences in LAI between leaf out and leaf drop; or by hemispherical photographs. Destructive sampling and allometric methods usually produce a constant ratio and can fail to reflect the variability of woody-to-total area ratio from one stand to another, depending on the stand age, location and growing situation. Although near-infrared hemispherical photos show the potential to derive the wood-to-total area ratio (Chapman, 2007), the contrast between woody structure and foliage is significantly influenced by the light conditions at the time of the hemispherical photo.

However, Echidna lidar records the full reflected waveform, providing information on the scattering properties of targets. Woody structure, foliage, and sky demonstrate varying scattering properties of total power, width, and location of the reflected pulse. The total power of the reflected pulse and its pulse width depends on several factors: the total power of transmitted pulse, the fraction of the laser pulse intercepted by the target, the variance in range in near-field scatterers (leaves) returning the pulse, the reflectance of the intercepted surfaces, and the fraction of illumination reflected back to the sensor. Pulses passing through the canopy into the sky return only system noise and so are easy to identify. Woody structures are identified using a threshold on the ratio of total power to reflected pulse width. Since trunks and branches are solid targets that reflect the incoming pulse strongly, they produce a sharply peaked return pulse. In contrast, lower power and a wider pulse, often with multiple pulses following, identifies foliage. Finally, ground reflections are identified by the elevation of the return pulse. Using these principles, Echidna lidar shots can be classified in into four components: sky, woody structures, foliage, and ground.

Fig. 2b shows a representative image showing these four classes. It demonstrates the potential to separate much of the foliage from woody structures, particularly for close targets where the pulse is of

smaller diameter. As the diameter of the pulse increases with range, the return is more likely to mix leaves and branches and thus the detection of trunks and branches is range-dependent. Although it should be possible to develop a range-dependent theoretical approach to estimate the proportions of woody and leafy material within a scan, we simply used a range-independent threshold to separate branches and foliage for this example.

Although this approach would have allowed correction of LAI values for near-field trunks and branches, we used both types of shots (woody and foliage) in deriving gap probabilities so that our effective LAI values could be compared directly with those of the LAI-2000 and hemispherical photos.

2.8. LVIS- vs. EVI-retrieved canopy height

Defined as "the vertical distance between the ground level and tip of the tree" in the forestry context (Husch et al., 1972), tree height is a key indicator of the amount of its above-ground biomass, and the range of tree heights within a stand is also a useful indicator of forest age and habitat quality. A number of studies have used airborne, nadir-looking lidar to retrieve tree and canopy heights from both small-footprint laser altimeters and large-footprint, waveform-digitizing lidar sensors (Lefsky et al., 1999a, 1999b; Harding et al., 2001; Hudak et al., 2002; Wulder et al., 2007). Most recently, Hilker et al. (2010) compared EVI scan data with small-footprint airborne lidar returns for four Douglas fir stands in British Columbia and reported good agreement (<2.5 m for heights of 35–40 m) between both maximum and dominant stand heights obtained using the two methods.

Canopy height is a structural parameter that requires careful definition. Typically it is taken as the mean height of "dominant" trees within a sample plot of fixed area. Where the canopy is dense and crowns are obscured, tree heights can be difficult to measure on the ground, even with an accurate hypsometer. Using a large-footprint airborne lidar to detect the top of the canopy, the return pulse will need to reach a level significantly exceeding the noise level, which requires a certain minimum of volume scattering material. The height at which this minimum volume is sensed will be somewhat below the tips of the dominant trees. It will also vary with the shape and scattering properties of the tip. That is, the heights of conifers, given their narrow tips and shoots, may be seen as somewhat lower than those of broadleaf trees, which typically have larger leaves and more closely-spaced twigs at the top as well as a broader crown shape.

To estimate stand height from EVI data, we used gap probability profiles derived from zenith rings for which lidar pulses can exit the canopy while still remaining within sensing range (usually $\leq 60°$). To determine the canopy height for the zenith ring, the gap probability is traced backward from a height above the canopy until a small variance is detected (set at 0.01 of the standard deviation of the P_{gap} values with distance for the zenith ring). The canopy mean top height (CMTH) is then taken as the average of these heights over the zenith rings, weighted by the solid angle associated with the zenith ring.[2]

We compared EVI canopy mean top heights to heights of returns obtained from the Lidar Vegetation Imaging Sensor (LVIS), an airborne, large-footprint, near-infrared scanning lidar that digitizes the full return waveform (Blair, et al., 1999). We used LVIS data acquired by aircraft overflights in 2003. Footprints were nominally spaced at 20 m and centers were geolocated within 1 m (Hofton et al., 2000). We used the RH100 parameter, obtained from the digitized return waveform, to represent the canopy height. This parameter provides the height that includes 100% of the scattered return exceeding a small noise threshold. LVIS data were available at 27 of the 29 plots for which CMTH values were available. To determine the RH100 value for the plot, we averaged RH100 values for all footprints with centers falling within 20 m of the plot center. The number of such footprints varied from 2 to 14, depending on the plot.

[2] The trees measured were a random sample of the sizes of all of the trees, producing an insufficient number of dominants for stand height determination.

3. Results

3.1. LAI comparisons

To assess the consistency of effective LAI retrievals using the four methods, we compared LAI results at both site scale and plot (scan) scale. At the plot scale, we averaged the 13 values obtained by the LAI-2000 and hemispherical photographs to provide a single value for each plot, ignoring variance at this lowest level of data structure.

Fig. 3 shows how effective LAI retrievals at plot level correlate with each other. All correlations are significant at the 99% level or higher, showing that all methods detect the same trend. However, there is substantial variation from method to method. The highest correlation is between the two types of EVI retrievals ($R^2 = 0.69$), which is not surprising since both are derived from the same data source. The R-squares between remaining pairs of methods range from 0.23 to 0.41, showing that each measurement technique provides a somewhat different result, even though all are based on the same optical principles using gap probability and centered at the same location.

Table 2 presents mean effective LAI values for each site. The means vary within a range of about 4 to 5, except for the Howland shelterwood site, where recent selective cutting has left the LAI somewhat lower. Standard deviations within sites largely fall within the range of about 0.2 to 0.8 units. This variance is probably due to two sources: variance within and across the techniques as discussed above and natural variance in the vegetation cover at plots within the same sites. As a reference, random errors observed by independent collaborators using repeated 100 m LAI-2000 transects at Bartlett and Howland were ± 0.30 units and systematic errors were ± 0.20 units.

To test our hypothesis that the effective LAI retrievals from EVI data are not statistically different from those obtained by other methods, we carried out pairwise analysis of variance (ANOVAs) tests. The specific structure was a three-way nested ANOVA, with factors of method (2), site (6), and plot (28) nested within site. In no cases were the means for the sites significantly different, so in each case, the null hypothesis is accepted.

Table 3 shows values for β, which is the probability of Type II error (accepting the null hypothesis when in fact it is false) for these comparisons as computed *a posteriori*. (The power of the test is equal to $1-\beta$.) The tests are most powerful for separating hemispherical photos from Echidna retrievals, and slightly less powerful for separating LAI-2000 and EVI retrievals. Except for the comparison between LAI-2000 and Echidna hinge angle LAI ($\beta = 0.154$), powers exceed 0.9. Thus, we can be reasonably confident that the Echidna retrievals are not significantly different from the others given the data at hand. We can also conclude that the LAI-2000 and hemispherical photos are similar with a power of 0.95.

In comparing the two EVI retrieval methods to each other, we conclude that they are not significantly different, although the power of the comparison test is somewhat lower than the others, at about 0.75. This reflects the strong correlation between the two sets of retrievals ($R^2 = 0.69$) that arises because both are derived from identical scans. As shown in Fig. 3, hinge angle correlations with LAI-2000 and hemispherical photos are slightly higher than those using the regression method, but it would be premature to conclude that the hinge angle method better fits the other methods. *A priori*, the regression method should be more robust since it uses zenith rings from 5° to 65° while the hinge angle method uses only a single zenith ring. Future work may resolve this issue.

Independent LAI retrievals (Table 2) also fall within the same range as ours. At Bartlett site, LAI-2000 data were collected within a few weeks of our scans by our collaborators. These LAIs, which

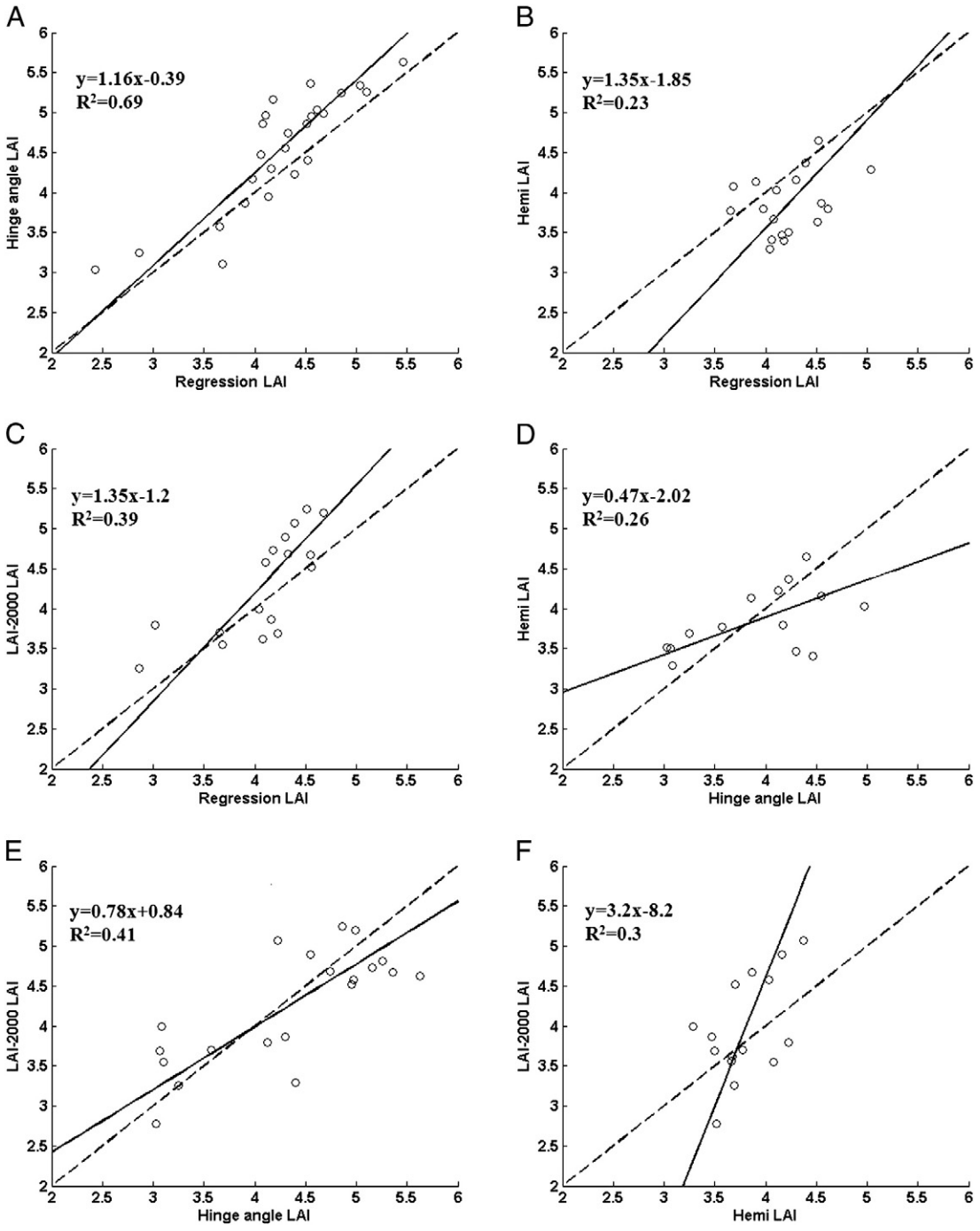

Fig. 3. Reduced major axis regression of regression LAI, hinge angle LAI, LAI from hemispherical photos, and LAI from LAI-2000. Subpanels A-F demonstrate the correlations among these four LAI retrievals.

covered a slightly different area, were slightly higher, but with overlapping standard deviations that were of about the same magnitude. Both measurements showed LAIs for site B2 about 0.5 units higher than site C2. Our foliage profiles also show that the canopy at site B2 is about 3 m taller, which may account for this difference. At the Howland Tower site, data were acquired from the prior year using the LAI-2000 (J. Lee, personal communication). Again, the standard deviation is similar and the mean value lies within the range of our retrievals. At Harvard, Cohen et al. (2006) observed an average value for the forest as a whole in summer 2000 and 2001 using LAI-2000 that is somewhat higher than we observed at our sites. Their standard deviation is also somewhat larger since it includes plots over the entire range of stands. Catovsky and Bazzaz (2000) estimated the LAI of a Harvard hemlock stand destructively, providing a single direct measurement value that lies in the middle of our range of retrievals.

3.2. Height comparisons

Fig. 4 graphs canopy mean top height (CMTH) retrieved with the EVI against LVIS RH100 values at the plot level. The slope and intercept are determined using reduced major axis regression (Kermack & Haldane, 1950), which is appropriate for a situation in which the independent variable is not under the control of the investigator (Curran & Hay, 1986; Davis, 1986; Miller & Kahn, 1962).

Table 2
Mean effective leaf area index retrievals with standard deviations, New England forest sites, 2007.

Site name	Bartlett		Harvard		Howland	
	B2	C2	Hardwood	Hemlock	Tower	Shelterwood
Site type	Hardwood	Hardwood	Hardwood	Conifer	Conifer	Conifer
EVI LAI, hinge angle	4.95[a]	3.90	4.45	4.85	5.25	3.75
	0.29[b]	0.52	0.83	0.51	0.39	0.29
EVI LAI, regression	4.60	4.23	4.16	4.47	4.80	3.74
	0.27	0.24	0.11	0.46	0.69	0.87
LAI-2000, BU	4.76	4.34	4.37	4.70	4.07	3.42
	0.96	1.04	0.14	0.04	0.51	0.41
LAI-2000, UHN[c]	5.03	4.55				
	0.36	0.29				
Hemispherical photographs	3.92	4.17	3.46	3.66	3.52	3.86
	0.29	0.49	0.34	0.22	0.26	0.29
LAI-2000, others			5.25[d]	4.4[e]	4.18[f]	
			0.82		0.45	

[a] Mean of 5 scans or plots at each site.
[b] Standard deviation.
[c] Transects very close to scans, but not centered on them.
[d] Cohen et al., 2006, all Harvard Forest.
[e] Destructive sampling, general value for hemlock at Harvard Forest; no standard deviation (Catovsky & Bazzaz, 2000).
[f] J. T. Lee, University of Maine.

Ninety-five percent confidence intervals on the slope [0.66, 1.21] and intercept [−3.61, 8.66] include the values 1 and 0; the specific values show that the observed regression line parallels the 1:1 line quite well with an offset of 1.2 m at the joint mean. Root mean squared error (RMSE) is 2.31 m, which is 9.9% of the mean of the RH100 values.

The mean deviation between the two sets of values is 1.14 m, with EVI values lower than LVIS. Should this trend prove significant in later trials, it would suggest that the mean canopy top height as measured by the EVI is different from mean RH100 values obtained from LVIS. This result could be explained by at least two factors. First, the LVIS and EVI canopy heights are measured at slightly different points on the return scattering profile and the profiles are derived in different ways, with the LVIS looking downward toward nadir from above and the EVI looking upward from below at zenith angles ranging up to 60°. Secondly, the absolute height measurements of either instrument may contain a small bias, for example due to instrument calibration. Mound-and-pit microtopography may also add variance by locally varying the ground height seen by LVIS or influencing the location at which the EVI instrument is above the forest floor.

Although the R^2 value for the regression is significant at the 99% level, its value, 0.439, shows significant unexplained variance between LVIS and EVI observations. In general, the values farthest below the line are conifer sites, while the outliers farthest above are hardwood sites. Inspection of the data shows that the mean deviation of hardwood sites from the regression line is +0.78 m, with RH100 values greater than Echidna CMTH values, and the mean deviation for conifer sites is −0.85 m, with RH100 values smaller than CMTH values. This suggests that the two sensing methods may respond differently to the difference in tree form, i.e., conifer or broadleaf.

3.3. Foliage profiles

Fig. 5 shows the foliage profiles retrieved from EVI observations for the six sites, grouped into hardwood and conifer types. Each profile is an average of the profiles of the five scans made at each site. The profiles are normalized to the total leaf area index retrieved using the Echidna regression method. Also, leaf area begins at instrument height, about 1.6 m, so a small amount of shrub understory below that level is not measured.

Among the hardwood sites, Harvard hardwood is the tallest, with its peak leaf area encountered at about 22 m. The understory is fairly open, with LAI deceasing smoothly from upper canopy to ground. Bartlett B2 shows its maximum leaf area in a broader belt from about 13 to 18 m with a second understory peak at about 5 m. Bartlett C2 is the shortest of the three stands and its peak leaf area is encountered at a height of only 11 m. Field measurements of mean stem diameter are about 2 cm smaller here than at the other two stands, and stand basal area is about 15% lower. The long slope from the top of the canopy (approximately 25 m) to the maximum (approximately 11 m) indicates that the foliage volume steadily increases to the maximum, which might be explained by a wider range of tree heights within the stand. There is also a minor shrub layer peak at about 3 m.

The conifer sites all show sharply peaked foliage profiles with little understory. From the top down, the curves appear to fit a model of leaf area that increases with crown width until the crowns touch and intersect, when leaf area is at its peak. Below that level, the crowns begin to thin, losing branches with age, and leaf area decreases quite

Table 3
Type II error probabilities (β) for pairwise ANOVAs.

Method	EVI LAI, regression	Hemispherical photographs	LAI-2000
EVI LAI, hinge angle	0.243	0.002	0.154
EVI LAI, regression		0.007	0.085
Hemispherical photographs			0.046

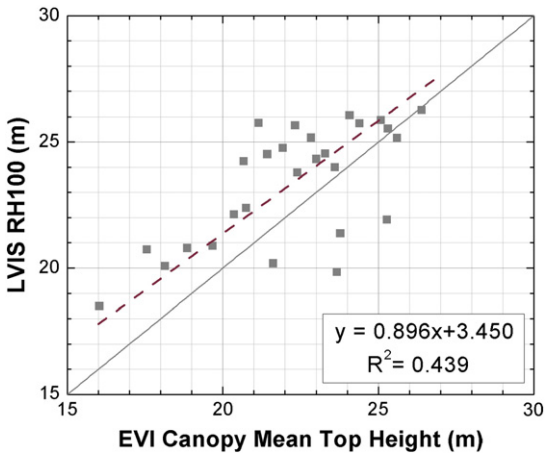

Fig. 4. Reduced major axis regression of LVIS and. Echidna canopy height estimations; 27 plots at six New England sites.

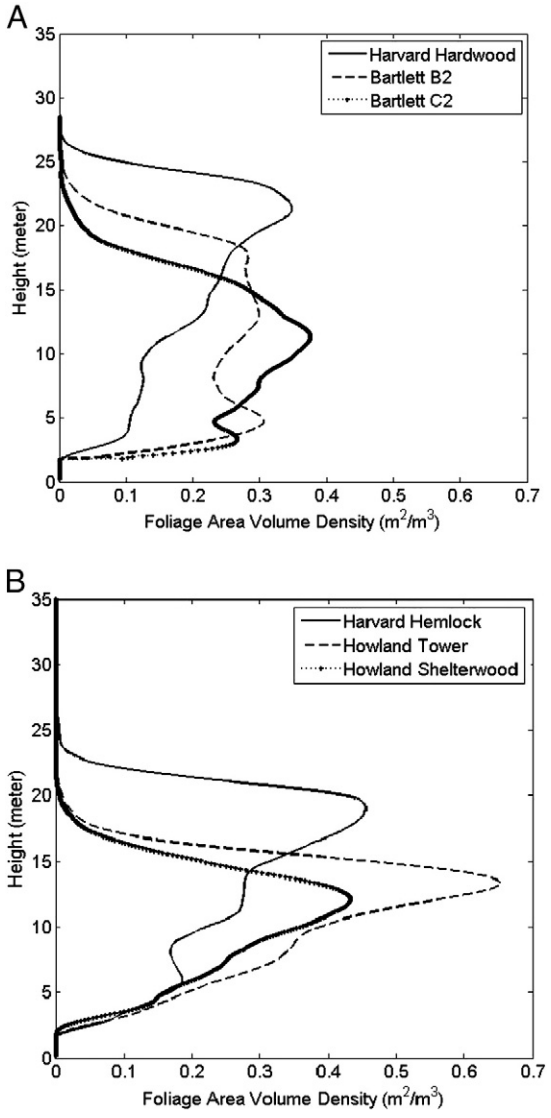

Fig. 5. Vertical foliage profiles for hardwood (A) and conifer sites (B). Each foliage profile is an average of 5 EVI scans for that site; each scan is based on about 400,000 lidar pulses exiting the canopy over an area of about 0.85 ha.

linearly to ground level. Of the three stands, Harvard hemlock is the tallest and reaches its peak leaf area at about 20 m. Field measurements of this stand show a mean diameter of about 20 cm. The Howland tower site, a stand of mixed-aged red spruce, shows leaf area sharply peaked at about 13 m. Here the mean diameter is 12 cm and the stocking is much denser than at Harvard hemlock, with about 2.5 times as many stems per hectare. At the Howland shelterwood stand, selective cutting has removed many of the larger trees, leaving a leaf area peak at only about 13 m, below that of the tower red spruce stand, in spite of a larger mean diameter (about 17 cm) for the remaining trees.

4. Discussion

Leaf area index is a biophysical parameter of vegetation that is used in many applications, ranging from modeling surface energy balance to carbon cycling. However, it is difficult to measure accurately. Destructive sampling, while potentially most accurate, is costly and requires careful sampling techniques. Optical methods using gap probability are widely used, but are limited by intrinsic problems of accounting for clumping of leaves and crowns and variation in leaf angle distribution. In this study, we do not have a "ground truth" component of direct LAI measurements that are inherently more accurate than indirect optical methods. As a result, we cannot conclude that any one optical method is more accurate than another—just that the methods all provide statistically equivalent measurements, given the inherent variance in the stands and techniques.

Determination of the most accurate optical technique would require significant modifications of our experimental design. First, reference measurements of LAI, probably using destructive sampling after acquisition of optical data, would be needed, including the variance in such measurements. Second, the selection of sites would have to include a full range of LAI values to permit regression analyses. Third, a more thorough sample design would be needed to establish sample variances at multiple levels, from the repeatability of individual measurements under varying environmental conditions to the spatial variance induced by the heterogeneous nature of the forest canopy and autocorrelation among optical samples having overlapping fields of view. Finally, sample sizes and protocols would need to be worked out from initial variance estimates and target confidence levels to assure significant results. Although desirable, an experiment of this nature would have required a level of effort well beyond that available to us.

Although we cannot conclude from our analysis that the EVI produces better LAI estimates, from first principles we might expect that full-waveform lidar overcomes some of the limitations of hemispherical photography and the LAI-2000. For example, classification of return pulses into tree or branch and leaf hits allows direct removal of the larger trunks and branches from the LAI retrieval. Also, as an active scanner, lidar is not sensitive to variations in sky brightness that can affect hemispherical photography and LAI-2000 observations and limit data acquisition to clear skies without direct solar illumination. Whether these strengths actually produce better data is yet to be determined.

In this study, we retrieved leaf area index from EVI scans by using gap probability in the far field, similar to hemispherical photography and the LAI-2000. However, lidar adds a third dimension to the data—the distance to each scattering event. Utilization of this third dimension opens the door to a number of innovative approaches to retrieving canopy structure that are currently under development.

One of these is better characterization of clumping within the canopy. Because the range to each hit is known, the angular width of a gap seen in a zenith ring can be converted to a physical width, allowing gap length statistics to separate within-crown and between-crown gaps more accurately. Gap length distributions could also be observed directly by range values from the instrument to the first hit and between multiple hits along a single pulse return.

In addition, the direction and range to each scattering event can be converted to a cloud of points in Cartesian coordinates, and overlapping scans from nearby locations can be merged to form 3-D reconstructions of stand segments (Yang et al., personal communication). From these, clumps and gaps could be directly observed and measured.

Another application is topographic correction of LAI estimates. Here, detailed topographic information derived from a point cloud could be used to level the canopy to a common datum before extracting LAI and the foliage profile.

Stand height is a parameter that is quite useful to modelers but, like LAI, is difficult to measure. It can be defined in a number of ways, for example as the mean height of the tallest trees (emergents); of dominant trees (crowns exposed to sun on all sides); or all trees above a specified diameter with intact crowns. The height of individual trees can be determined quite accurately using optical instruments or laser rangefinders if both the top and base of the tree are visible from a distance about equal to the height. However, these conditions are not always met for every tall tree in a stand.

Large-footprint, above-canopy lidars, like the LVIS, provide a composite measurement of the height of trees with a footprint of 15–30 m diameter that will be different from, but strongly related to, manual measurements. The foliage profile retrieved by the EVI also provides stand height, but from a different perspective and over a somewhat larger area than a single lidar footprint. The LVIS sees height from nadir and RH100 is sensitive to both the shape of the tree crowns and their location within the footprint, which tends to be center-weighted (R. Dubayah, personal communication).

In comparison, the EVI foliage profile that is used to determine stand height is retrieved from many pulses that exit the canopy at many upward angles. Based on this more comprehensive information, the EVI measurement is likely to have lower variance and be less influenced by the shape of the tree crowns at the site. However, the ground measurement characterizes only a single stand at a time, while the LVIS can map large areas. In practice, the two instruments could be used synergistically to good effect, not only for height retrieval, but also to calibrate foliage profiles derived from vertical LVIS waveforms (Ni-Meister et al., 2008).

5. Conclusions

This study shows that the Echidna Validation Instrument (EVI) can provide measurements of effective LAI that are statistically similar to those using hemispherical photography or the LAI-2000 instrument; provide canopy heights that are comparable to RH100 values from LVIS; and retrieve foliage profiles that are consistent with what is known about the structure of the stands we selected.

Although the EVI is a prototype, it points the way to rapid and cost-effective assessment of leaf area index, foliage profile, and canopy height. Coupled with retrievals of mean diameter at breast height, stem count density, basal area, and above-ground woody biomass (Yao et al., 2011), full-waveform ground-based lidar provides a methodology that should be able to measure forest structure more rapidly and with less field effort than standard forestry methods. Moreover, merging multiple overlapping scans to create a point cloud that reconstructs the forest in *x, y, z*-space opens another door to many new approaches to measure forest structure.

Acknowledgments

This research was supported by NASA under grants NNG06GI92G and NNX08AE94A and NSF under grant 0923389. The authors gratefully acknowledge the assistance of John Lee at Howland Experimental Forest and Audrey Barker Plotkin at Harvard Forest. Co-author Richardson acknowledges support from the U.S. Department of Energy's Office of Science (BER) through the Northeastern Regional Center of the National Institute for Climatic Change Research, the Terrestrial Carbon Program under interagency agreement No. DE-AI02-07ER64355, and the Carbon Sequestration Program under award number DE-FG02-00ER63001. Shihyan Lee helped by providing information based on LVIS data for our height validations. We are also grateful to the many suggestions made by reviewers that significantly improved our paper.

References

Andrieu, B., Sohbi, Y., & Ivanov, N. (1994). A direct method to measure bidirectional gap fraction in vegetation canopies. *Remote Sensing of Environment*, *50*, 61–66.

Blair, J. B., Hofton, M. A., & Rabine, D. L. (2006). Processing of NASA LVIS elevation and canopy (LGE, LCE and LGW) data products, version 1.01. Available at:. http://lvis.gsfc.nasa.gov

Blair, J. B., Rabine, D. L., & Hofton, M. A. (1999). The Laser Vegetation Imaging Sensor (LVIS): A medium-altitude, digitization-only, airborne laser altimeter for mapping vegetation and topography. *ISPRS Journal of Photogrammetry and Remote Sensing*, *54*, 115–122.

Breda, N. J. (2003). Ground-based measurements of leaf area index: A review of methods, instruments and current controversies. *Journal of Experimental Botany*, *54*, 2403–2417.

Campbell, G. S. (1986). Extinction coefficients for radiation in plant canopies calculated using an ellipsoidal inclination angle distribution. *Agricultural and Forest Meteorology*, *36*, 317–321.

Catovsky, S., & Bazzaz, F. A. (2000). Contributions of coniferous and broad-leaved species to temperate forest carbon uptake: A bottom-up approach. *Canadian. Journal of Remote Sensing*, *30*, 100–111.

Chapman, L. (2007). Potential applications of near infra-red hemispherical imagery in forest environments. *Agricultural and Forest Meteorology*, *143*(1–2), 151–156.

Chen, J. M., & Black, T. A. (1992). Foliage area and architecture of plant canopies from sunfleck size distributions. *Agricultural and Forest Meteorology*, *60*(3–4), 249–266.

Chen, J. M., & Cihlar, J. (1995). Quantifying the effect of canopy architecture on optical measurements of leaf area index using two gap size analysis methods. *IEEE Transactions on Geoscience and Remote Sensing*, *33*, 777–787.

Chen, J. M., Govind, A., Sonnentag, O., Zhang, Y., Barr, A., & Amiro, B. (2006). Leaf area index measurements at Fluxnet Canada forest sites. *Agricultural and Forest Meteorology*, *140*, 257–268.

Chen, J. M., Rich, P. M., Gower, S. T., Norman, J. M., & Plummer, S. (1997). Leaf area index of boreal forests: Theory, techniques, and measurements. *Journal of Geophysical Research*, *102*(D24), 429–443.

Clark, D. B., Olivas, P. C., Oberbauer, S. F., Clark, D. A., & Ryan, M. G. (2008). First direct landscape-scale measurement of tropical rain forest Leaf Area Index, a key driver of global primary productivity. *Ecology Letters*, *11*, 163–172.

Cohen, W. B., Maiersperger, T. K., Turner, D. P., Ritts, W. D., & Pflugmacher, D. (2006). MODIS land cover and LAI collection 4 product quality across nine states in the western hemisphere. *IEEE Transaction on Geosciences and Remote Sensing*, *44*(7), 1843–1856.

Curran, P., & Hay, A. (1986). The importance of measurement error for certain procedures in remote sensing at optical wavelengths. *Photogrammetric Engineering and Remote Sensing*, *52*, 229–241.

Davis, J. (1986). *Statistics and data analysis in geology (2nd edition)*. New York: John Wiley & Sons.

Frazer, G. W., Fournier, R. A., Trofymow, J. A., & Hall, R. J. (2001). A comparison of digital and film fisheye photography for analysis of forest canopy structure and gap light transmission. *Agricultural and Forest Meteorology.*, *2984*, 1–16.

Hale, S. E., & Edwards, C. (2002). Comparison of film and digital hemispherical photography across a wide range of canopy densities. *Agricultural and Forest Meteorology*, *112*, 51–56.

Harding, D. J., Lefsky, M. A., Parker, G. G., & Blair, J. B. (2001). Laser altimeter canopy height profiles: Methods and validation for deciduous, broadleaf forests. *Remote Sensing of Environment*, *76*(3), 283–297.

Helena, E., Lars, E., Karin, H., & Anders, L. (2005). Estimating LAI in deciduous forest stands. *Agricultural and Forest Meteorology*, *9*(2), 27–37.

Hilker, T., van Leeuwen, M., Coops, N. C., Wulder, M. A., Newnham, G. J., Jupp, D. L. B., et al. (2010). Comparing canopy metrics derived from terrestrial and airborne laser scanning in a Douglas-fir dominated forest stand. *Trees*, *24*, 819–832.

Hofton, M. A., Blair, J. B., Minster, J. B., Ridgway, J. R., Williams, N. P., Bufton, J. L., et al. (2000). An airborne scanning laser altimetry survey of Long Valley, CA. *International Journal of Remote Sensing*, *21*, 2413–2437.

Hudak, A. T., Lefsky, M. A., Cohen, W. B., & Berterretche, M. (2002). Integration of lidar and Landsat ETM+ data for estimating and mapping forest canopy height. *Remote Sensing of Environment*, *82*(2–3), 397–416.

Husch, B., Miller, C., & Beers, T. (1972). *Forest mensuration* (2th ed.). New York: Ronald Press Company.

Hyde, P., Dubayah, R., Walker, W., Blair, J. B., Hofton, M., & Hunsaker, C. (2006). Mapping forest structure for wildlife habitat analysis using multi-sensor (lidar, SAR/INSAR, ETM+, quickbird) synergy. *Remote Sensing of Environment*, *102*(1–2), 63–73.

Jensen, L. R., Humes, K. S., Vierling, L. A., & Hudak, A. T. (2008). Discrete return Lidar-based prediction of leaf area index in two conifer forests. *Remote Sensing of Environment*, *112*(10), 3947–3957.

Jonckheere, I., Fleck, S., Nackaerts, K., Muys, B., Coppin, P., Weiss, M., et al. (2004). Review of methods for in situ leaf area index determination: Part I. theories, sensors and hemispherical photography. *Agricultural and Forest Meteorology*, *121*(1–2), 19–35.

Jonckheere, I., Nackaerts, K., Muys, B., & Coppin, P. (2005). Assessment of automatic gap fraction estimation of forests from digital hemispherical photography. *Agricultural Forest Meteorology*, *132*, 96–114.

Jupp, D. L. B., Culvenor, D. S., Lovell, J. L., & Newham, G. J. (2005). *Evaluation and validation of canopy laser radar (LIDAR) systems for native and plantation forest inventory*. CSIRO Marine and Atmospheric Research, Canberra, Australia. CSIRO Marine and Atmospheric Research Paper 020 Available at. http://www.cmar.csiro.au/publications/cmarseries/rame.html

Jupp, D. L. B., Culvenor, D. S., Lovell, J. L., Newnham, G. J., Strahler, A. H., & Woodcock, C. E. (2009). Estimating forest LAI profiles and structural parameters using a ground based laser called "Echidna®". *Tree Physiology*, *29*(2), 171–181.

Jupp, D. L. B., & Lovell, J. L. (2007). *Airborne and ground-based lidar systems for forest measurement: Background and principles*. CSIRO Marine and Atmospheric Research, Canberra, Australia. CSIRO Marine and Atmospheric Research Paper 017 Available at. http://www.cmar.csiro.au/publications/cmarseries/frame.html

Kermack, K. A., & Haldane, J. B. S. (1950). Organic correlation and allometry. *Biometrika*, *37*, 30–41.

Lang, A. R. G. (1987). Simplified estimate of leaf area index from transmittance of the sun's beam. *Agricultural and Forest Meteorology.*, *41*, 179–186.

Lang, A. R. G., & Xiang, Y. (1986). Estimation of leaf area index from transmission of direct sunlight in discontinuous canopies. *Agricultural and Forest Meteorology*, *37*, 229–243.

Leblanc, S. G. (2002). Correction to the plant canopy gap size analysis theory used by the tracing radiation and architecture of canopies (TRAC) instrument. *Applied Optics*, *31*(36), 7667–7670.

Leblanc, S. G., Chen, J. M., Fernandes, R., Deering, D. W., & Conley, A. (2005). Methodology comparison for canopy structure parameters extraction from digital hemispherical photography in boreal forests. *Agricultural and Forest Meteorology*, *129*(3–4), 187–207.

Lefsky, M., Cohen, W., Acker, S., Parker, G., Spies, T., & Harding, D. (1999a). Lidar remote sensing of biophysical properties and canopy structure of forests of Douglas-fir and western hemlock. *Remote Sensing of Environment*, *70*(3), 339–361.

Lefsky, M., Harding, D., Cohen, W., Parker, G., & Shugart, H. (1999b). Surface lidar remote sensing of basal area and biomass in deciduous forests of eastern Maryland, USA. *Remote Sensing of Environment*, *67*(1), 83–98.

Magnussen, S., & Boudewyn, P. (1998). Derivations of stand heights from airborne laser scanner data with canopy-based quantile estimators. *Canadian Journal of Forest Research*, *28*, 1016–1031.

Miller, J. B. (1967). A formula for average foliage density. *Australian Journal of Botany*, *15*, 141–144.

Miller, R., & Kahn, J. (1962). *Statistical analysis in the geological sciences.* New York: John Wiley & Sons.

Morsdorf, B., Kotz, E., Meier, K. I., & Allgower, B. (2006). Estimation of LAI and fractional cover from small footprint airborne laser scanning data based on gap fraction. *Remote Sensing of Environment*, *104*, 50–61.

Myneni, R. B., Hoffman, S., Knyazikhin, Y., Privette, J. L., Glassy, J., Tian, Y., et al. (2002). Global products of vegetation leaf area and fraction absorbed PAR from year one of MODIS data. *Remote Sensing of Environment*, *83*, 214–231.

Ni-Meister, W., Strahler, A. H., Woodcock, C. E., Schaaf, C. B., Jupp, D. L. B., Yao, T., et al. (2008). Modeling the hemispherical scanning, below-canopy lidar and vegetation structure characteristics with a geometric-optical and radiative-transfer model. *Canadian Journal of Remote Sensing*, *34*(2), 385–397.

Parker, G. G., Harding, D. J., & Berger, M. (2004). Portable LIDAR system for rapid determination of forest canopy structure. *Journal of Applied Ecology*, *41*, 755–767.

Riańo, D., Valladares, F., Condes, S., & Chuvieco, E. (2004). Estimation of leaf area index and covered ground from airborne laser scanner (lidar) in two contrasting forests. *Agricultural and Forest Meteorology*, *124*, 269–275.

Ross, J. (1981). *The radiation regime and architecture of plant stands.* Boston: Dr. W. Junk Publishers.

Strahler, A. H., Jupp, D. L. B., Woodcock, C. E., & Schaaf, C. B. (2008). Retrieval of forest structure parameters using a ground based laser instrument (Echidna®). Special issue for. *Canadian Journal of Remote Sensing*, *34*(2), 426–440.

Wagner, S. (2001). Relative radiance measurements and zenith angle dependent segmentation in hemispherical photography. *Agricultural Forest Meteorology*, *107*(2), 103–115.

Walter, J. M., & Torquebiau, E. (2000). The computation of forest leaf area index on slope using fish-eye sensors. *Compte-Rendu de l'Académie des Sciences, Paris. Life Sciences*, *323*, 801–813.

Weiss, M., Baret, F., Smith, G. J., Jonckheere, I., & Coppin, P. (2004). Review of methods for in situ leaf area index (LAI) determination: Part II. estimation of LAI, errors and sampling. *Agricultural and Forest Meteorology*, *121*(1–2), 37–53.

Welles, J. M., & Norman, J. M. (1991). Instrument for indirect measurement of canopy architecture. *Agronomy Journal*, *83*, 818–825.

Wilson, J. W. (1963). Estimation of foliage denseness and foliage angle by inclined point quadrats. *Australian Journal of Botany*, *11*, 95–105.

Wulder, M. A., Tian, H., Joanne, C. W., Tatsuo, S., & Hayato, T. (2007). Integrating profiling LIDAR with Landsat data for regional boreal forest canopy attribute estimation and change characterization. *Remote Sensing of Environment*, *110*, 123–137.

Yao, T., Yang, X. Y., Zhao, F., Wang, Z. S., Zhang, Q. L., Jupp, D. L. B., Culvenor, D. S., Newnham, G. J., Ni-Meister, W., Schaaf, C. B., Woodcock, C. E., & Strahler, A. H. (2011). Measuring forest structure and biomass in New England forest stands using Echidna ground-based lidar. *Remote Sensing of Environment*, *115*, 2965–2974 (this issue).